Macromolecules
ARTICLE

Macromolecules **2010**, *43*, 10505–10511 **10505**
DOI: 10.1021/ma1022692

Free Volume of Interphases in Model Nanocomposites Studied by Positron Annihilation Lifetime Spectroscopy

Stephan Harms, Klaus Rätzke,* and Franz Faupel

Institut für Materialwissenschaft, Materialverbunde, Technische Fakultät, Christian-Albrechts Universität zu Kiel, 24143 Kiel, Germany

Gerald J. Schneider, Lutz Willner, and Dieter Richter

Institut für Festkörperforschung, Neutronenstreuung and Jülich Centre for Neutron Science, Forschungszentrum Jülich, D-52425 Jülich, Germany

Received October 2, 2010; Revised Manuscript Received November 19, 2010

ABSTRACT: The free volume studies were performed in well characterized model nanocomposites by positron annihilation lifetime spectroscopy (PALS) to explore the influence of the interphase nanoscale character of the hydrophobically functionalized filler particles and the nanoscale particle size on positron parameters. A weakly repulsive system, which should not form an interphase, was obtained by mixing of low molecular weight poly(ethylene-*alt*-propylene) (PEP) and hydrophobically modified silica with varying concentration. A low molecular weight sample was chosen. Because of a finite centre of mass diffusion and a low radius of gyration the interstitials between particles are effectively filled and hence a most suitable model system is obtained. The absence of an interphase was confirmed by neutron scattering and neutron spin echo measurements. DSC experiments showed a constant glass transition temperature T_g and a decrease in Δc_p at T_g with increasing filler concentration as expected. In contrast, PALS measurements showed decreasing glass transition temperatures and a strong drop of the thermal expansion coefficient above T_g. These seemingly conflicting results are demonstrated to be due to nanoscale character of the hydrophobically functionalized filler particles with sizes in the range of the positronium diffusion length which requires taking into account out-diffusion of positronium from the particles. In particular, it is shown that the changes on PALS parameters such as *o*-Ps lifetime or its intensity, with increasing filler content cannot be attributed to the formation of an interphase with properties different from the polymer matrix. Like the neutron scattering experiments, PALS does not find any evidence of an interphase between the filler and the polymer within the resolution limit of the present technique, which is in agreement to the neutron scattering experiments.

Introduction

Polymer nanocomposites have been investigated intensively during the last decades due to a variety of applications.[1−3] They benefit particularly from the huge effective interfacial area resulting form the nanoscale size of the filler particles. The nanocompsosites usually consist of nanoparticles, covered with a functionalized shell to avoid agglomerations of particles and to avoid adsorption of polymer on particles. The particles together with functionalized shell will be termed as filler in this paper. In order to explain the macroscopic material behavior, a so-called interphase is frequently assumed.[4] It is proposed that the polymer in the vicinity of the particles (i.e., starting at the polymer−particle *interface*), generate such an interphase with properties different from the bulk. For example, if the chains adsorb on the surface, then interphases with higher density in comparison with the pure polymer melt are reported.[4] In the case of nonadsorbing chains a decreasing density is observed. For both cases, the properties of the polymer such as free volume, polymer dynamics and chain conformation are expected to deviate from bulk behavior.

Several properties like viscosity, permeability, toughness etc. are affected by the free volume.[5] However, only a few techniques such as *PVT* (pressure−volume−temperature) measurements,[6] Xe-129 NMR spectroscopy[7] and positron annihilation lifetime spectroscopy (PALS)[8,9] allow to determine the free volume hole sizes. A recent comparison on selected techniques is already reported in literature.[10,11] As the size of the holes which can be detected has to be larger than the probe size positron annihilation, which probes the electron density distribution and thus the free space between atoms is superior over the other techniques and most sensitive to subtle changes in free volume. The main point is that the *ortho*-positronium lifetime (*o*-Ps), i.e., the time between injection of the positron and the decay with the sample electrons, directly scales with the diameter of the free volume hole where it is located. PALS is now a well established technique for free volume investigations in polymers in general[8,9] and in polymeric membranes.[7,10,12,13] Once injected from a radioactive source, positrons form hydrogen-like positronium (Ps) states in most polymers, which are localized in defects with reduced electron density. The vacuum lifetime τ_3 of the *o*-Ps state of 142 ns is reduced in matter by the interaction with electrons from the wall of the free volume hole (pick-off annihilation), and is usually in the range of 1−10 ns for polymers.

Besides improvement of measurement technology, the well-known model developed by Tao[14] was crucial for applying PALS to study polymers. In this simple quantum mechanical model it is assumed that the Ps is confined to spherical holes with infinitely high walls. For such a problem, the Schrödinger equation can be

*Corresponding author. E-mail: kr@tf.uni-kiel.de. Telephone: +49-431-880-6227. Fax: +49-431-880-6227.

Published on Web 12/03/2010

solved analytically. Furthermore, the model postulates an electron layer at the pore wall, with which the *ortho*-Positronium can interact and decay. Calculation of the overlap integral of the positronium probability density function with this electron layer yields a direct relation between the positronium lifetime and the hole radius R_h as shown in eq 1.

$$1/\tau_3 = \lambda_0\left[1-\frac{R_h}{R_h+\Delta R}+\frac{1}{2\pi}\sin\left(\frac{2\pi R_h}{R_h+\Delta R}\right)\right] \quad (1)$$

This equation includes the reciprocal *ortho*-positronium decay rate $\tau_{o\text{-}Ps}$, the spin averaged decay rate in the electron layer λ_0, the hole radius R_h, and the thickness of the electron layer ΔR, which has been calibrated using substances with known pore sizes.[15] Since hole sizes in amorphous polymers are relatively broadly distributed, the discrete $\tau_{o\text{-}Ps}$ obtained from fits to lifetime spectra and hence the hole radius have to be regarded as average values,[16] and it is now common to use a software including a distribution of lifetimes σ.[17]

This technique has been applied several times to various polymers and polymer nanocomposites by the authors[13,18,19] and by others, e.g. refs 20 and 21. However, in the latter investigations, the focus was on the correlation of gas separation properties and the free volume like in the pioneering work by Merkel et al.[22] on this topic.

Systematic studies on polymer−nanocomposites have been performed, e.g., by Jean and co-workers. They reported lifetime spectroscopy measurements on polystyrene−silica nanocomposites,[24] considered as a weakly interacting system. From the changes in slope in the *o*-Ps vs temperature curve they deduce two separate glass transitions, where they attribute one of the glass transitions to the interphase.

PDMS silica−nanocomposites were investigated by Dlubek and co-workers.[25] However, only one concentration of filler was studied, and the focus of this paper was on the influence of cold crystallization and the correlation to the nanoparticles.

Interesting references for the present investigation are the papers by Winberg, Eldrup, and Maurer.[20,21,26] In particular they reported positron annihilation lifetime spectroscopy study on fumed SiO_2−PDMS nanocomposites.[20] Their DSC analysis shows a constant T_g and a decrease in Δc_p at the glass transition, with increasing filler concentration as expected from the decreasing polymer fraction. In their PALS experiments they observe a nonlinear relation between *o*-Ps intensity I_3 and filler concentration. In the *o*-Ps lifetime τ_3, a systematic decrease was observed at fixed temperature with increasing filler concentration (see Figure 4 of their paper). Their interpretation was centered around attractive filler−polymer interaction and the speculation that *o*-Ps may be able to diffuse out of the small nanoparticles.

In a similar investigation by these authors,[26] PTMSP-based nanocomposites with concentrations between 0 to 50% of hydrophobic fumed silica particles with an averaged diameter of 12 nm, were investigated. For the pure PTMSP, two long lifetimes (τ_3 and τ_4) were observed, whereas for the pure filler the contribution from particles (τ_3) and from interstitial cavities between the filler particles (τ_5), were determined. However, in the composites these contributions could not be clearly separated due to problems with fitting similar lifetimes. The longest lifetime τ_5, attributed to cavities between the filler particles, increased with filler concentration. This was attributed to less polymer being able to fill the increasingly smaller interstitial space between the particles. Whereas, the significant increase in τ_4 with filler concentration, even at low filler contents, was taken as an evidence that the filler surface induces significant changes in the polymer free volume even relatively far from the filler surface due to low flexibility of the backbone. The authors also speculate on nonequilibrium structures and it was also observed that the *o*-Ps intensities follow a mixing rule. Altogether the data show a good correlation between free volume and the permeability of gases. In the last paper of Winberg et al. on clay−polyamide 6 nanocomposites,[21] the focus is on relative changes of the amorphous to crystalline volume fraction. At high concentrations of clay (i.e., > 19 wt %) an increase in the free volume cavity diameter was observed, indicating a lower chain packing efficiency in the polyamide 6/clay nanocomposites.

In a recent paper, Harton et al.[27] combined PALS and DSC investigations on planar samples and poly(2-vinylpyridine) silica−nanocomposites (considered as a strongly interacting system), to detect changes of interphase width due to curvature. They indeed observe an increase in interphase width (termed bound layer by the authors) for nanoparticles. Positron lifetime experiments with a moderated beam have also been performed in the group of Y. C. Jean, who determined depth dependent glass transition temperatures from PALS experiments and interpreted this in terms of different degrees of free volume distributions at the surface and the interface.[28] They also investigated CO_2 pressurized carbon nanofiber-polystyrene nanocomposites and explained their results with compensation of stiffening the polystyrene by nanofibers and plasticizing by CO_2.[29]

It is obvious from the above discussion, that up to now no clear separation could be made between effects due to the interphase and due to the functionalized layer on the nanoparticle, which is necessary to avoid particle agglomeration and to avoid adsorption of polymer on particles. Therefore, it is the aim of the present work, to study a model nanocomposite without a significant interphase. Such a model system is obtained by mixing the hydrophobic poly(ethylene-*alt*-propylene) with silica particles with a hydrophobic surface coating. Thus, a system with essentially repulsive interactions is obtained. Only van der Waals interactions may lead to a very weak attractive contribution. For exactly the same system, neutron scattering experiments proved that a polymer interface layer—having different properties with respect to the bulk—surrounding the particles does not exist. In particular, small-angle neutron scattering experiments demonstrated that neither the chain conformation nor the radius of gyration of the polymer are changed neither in the bulk nor in the vicinity of the particle surface.[30] Therefore, a density change of the polymer due to the presence of the filler can be excluded. Furthermore, by neutron spin echo experiments it could be shown that all segments are equally mobile.[31,32] Concerning the PALS measurements, a further advantage of the present system is the low molecular weight of the polymer. On the one hand, the short polymer chains perform a finite center of mass diffusion.[33] On the other hand, the end-to-end distance R_E of the polymer is much smaller than the particle size. Thus, interstitial voids between the particles can be filled by the polymer offering the advantage that artifacts, e.g. due to unfilled cavities, are minimized. This would not be possible in the case of high molecular weight polymers, where the above-mentioned lifetime contributions from interstitial voids complicate the evaluation.[26] It is the aim of the present paper to report a systematic investigation on the strength and limitations of the PALS technique, for studying nanocomposites and to resolve conflicting results in literature. In particular, we demonstrate that PALS is very sensitive to the functionalized layer, and we conclude that in our system no significant interphase is formed.

Experimental Section

Sample Synthesis. The model nanocomposites studied in the present work consist of the nonpolar poly(ethylene-*alt*-propylene) (PEP) as the polymer component and a filler, consisting of silica nanoparticles (referred to as nanoparticle) with the surface

Table 1. Elemental Analysis of the Tol-St Particles

element	Si	O	H	C
mass fraction	0.46	0.45	0.01	0.08
number fraction	0.26	0.45	0.19	0.10

Table 2. Molecular Characteristics of PEP Polymers

sample	M_n	M_w/M_n
h-PEP3k	2980 (g/mol)	1.04
d-PEP3k	3400 (g/mol)	1.04

coated by short hydrocarbons from Nissan Chemical. Thus, nanocomposites with weak, essentially repulsive interactions are achieved. Nonrepulsive forces can occur only due to van der Waals attraction.

In order to resolve the contradictions raised in the literature, we studied one selected model nanocomposite with different techniques. Exactly the same samples were characterized by small-angle neutron scattering and neutron spin echo experiments.[30−32]

The silica nano fillers were obtained from Nissan Chemical (trade name: ORGANOSILICASOL Tol-St). The particle diameter supplied ranges from 10 to 15 nm. Approximately 20% of the OH surface groups were replaced by short hydrocarbons, which suffices to render the particle hydrophobic. The silica particles are supplied in a stable toluene solution at a particle fraction of 30 vol %. To obtain further information, elemental analysis was conducted,[30] yielding the element abundances given in Table 1.

The thickness of the functionalized surface layer is known from SANS measurements to be approximately 1.3 nm. The polymer matrix consists of hydrogenated and deuterated PEP with a ratio of 52/48, respectively. Corresponding neutron scattering experiments can be found elsewhere.[30−32] The PEP polymers were synthesized from parent polyisoprenes, h- and d-PI, by catalytic hydration (deuteration) using a conventional $Pd/BaSO_4$ catalyst. The corresponding polyisoprenes were prepared by anionic polymerization of isoprene (*d*-isoprene) monomer, with *tert*-butyllithium as initiator and benzene as polymerization solvent. Under these polymerization conditions the obtained microstructure typically consists of 75% *cis*-1,4, 18% *trans*-1,4, and 7% 3,4 units. The number-average molecular weight of the h-PI3k sample was obtained from ^{1}H NMR measurements using the 9 protons of the *tert*-butyl initiator group as internal reference. Size exclusion chromatography (SEC) on the d-PI3k and h-PI3k in tetrahydrofuran (THF) revealed almost identical elution volumes. The molecular weight of the d-PI3k is then derived from the number-average molecular weight of the h-PI3k obtained by NMR, multiplied by the ratio of the molecular weights of the monomeric units, 76/68. The polydispersity of all PIs were determined by SEC in THF relative to polystyrene standards. After saturation all PEP materials were remeasured by SEC revealing no detectable changes in polydispersity. For the h-PEP materials complete saturation was verified by the disappearance of the vinyl protons in the ^{1}H NMR spectra. Complete saturation was also assumed for the d-PEP polymers since they were prepared identically. The average molecular weights of the final PEP polymers were then recalculated by simply adding D_2 or H_2 per repeat unit. The characteristics of the PEP polymers are summarized in Table 2.

The nanocomposites consisted of the PEP described above and appropriate amounts of filler. The concentrations are given in volume % if not stated otherwise, hence 100% corresponds to the pure filler. Samples were obtained by means of solution mixing in toluene. After stirring for 48 h, the samples were first evaporated in air for 12 h and then dried in a vacuum oven for 48 h at $T = 50$ °C.

Differential Scanning Calorimetry (DSC). For thermal analysis a Perkin-Elmer Pyris DSC 1 apparatus was used with a heating rate 20 °C/min, and Argon as purge gas with a flow of 20 mL/min. Samples with weights of 9.87−10.71 mg were put into a 50 μL Al pan. Evaluation of data was done with the Pyris software, T_g determination of second heating run was determined by onset temperature. The error bar of ±2 °C comes from repeated measurements and evaluation uncertainties. Whereas, the Δc_p was calculated directly from the measurement curve with the built-in software, taking into account constant slope, therefore no direct error bar can be given. A rough estimate would be an error of 20% of the value. For the pure filler, no glass transition could be seen, probably due to the low amount of the functionalized hydrophobic shell polymer.

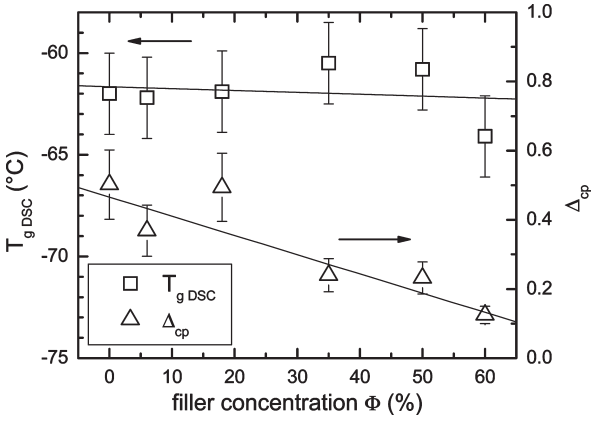

Figure 1. Summary of DSC experiments, glass transition temperature T_g (squares, left-hand scale) and Δc_p (triangles, right-hand scale) as a function of filler concentrations. The lines through the data result from a linear fit (see text for details and interpretation).

Positron Annihilation Lifetime Spectroscopy (PALS). Positron annihilation lifetime spectroscopy (PALS) measurements were performed in apparatus as described in previous papers[12,34] with standard ORTEC electronics and a homemade sample holder, while the time resolution was approx 235 ps. The samples were put into Al pans ($7 \times 7 \times 0.8$ mm^3), covered with Kapton foil (25 μm), a material which does not allow positronium formation. The source activity was ∼1MBq, resulting in a count rate of 400 cps, and in order to reduce the systematic error the same source was used for all samples. All spectra were counted to at least 5×10^6 counts at a background of ∼100 cts. For the evaluation we kept $\tau_1 = 125$ ps (p-Ps lifetime) constant and allowed free fit of all other lifetimes, dispersion and intensities. The resolution function was obtained from reference samples (high purity Silicon wafer) and was kept fixed for the complete series of evaluation. Special care was taken to avoid discrepancies due to different evaluation methods and only comparable data are presented in the following discussion. For the sample with 60% of filler and the pure filler (i.e., 100%) we added a long lifetime of several ns to take into account the voids between the filler particles. Vacuum during measurements was better than 10^{-5} mbar: After mounting at room temperature, a temperature scan was performed from −170 to +50 °C in steps of 10 °C, with a measurement accuracy of ±1 °C. In contrast to PDMS samples,[20,25] an equilibration was not necessary here, as the glass transition temperature of present polymer is below room temperature.

Results and Discussion

Differential Scanning Calorimetry (DSC). In Figure 1 the results of the DSC experiments are summarized. The glass transition temperature T_g is independent of the filler concentration within error bar, whereas the change of the heat capacity at T_g decreases monotonically with increasing filler concentration.

A simple mixing rule explains the data here. The T_g stays constant, as the volume contribution of the functionalized

Table 3. Complete Set of Results for Evaluation of PALS Spectra for All Concentrations for Two Different Temperatures

c_{filler} (%)	T (°C)	τ_2 (ns)	τ_3 (ns)	σ_3 (ns)	τ_4 (ns)	I_2 (%)	I_3 (%)	I_4 (%)
0	0	0.34	1.42	0.33		72.0	19.3	
6	0	0.34	1.38	0.33		76.1	17.7	
18	0	0.36	1.49	0.32		75.0	18.6	
35	0	0.37	1.56	0.38		71.5	21.8	
50	0	0.37	1.56	0.34		70.5	21.5	
60	0	0.40	1.77		21.4	71.7	15.9	1.8
100	0	0.47	2.44		66.2	51.7	6.1	11.0
0	120	0.35	2.41	0.69		62.7	21.5	
6	120	0.38	2.48	0.63		65.3	23.2	
18	120	0.40	2.56	0.69		68.0	22.2	
35	120	0.40	2.54	0.72		68.8	22.0	
50	120	0.40	2.35	0.68		69.4	21.5	
60	120	0.41	2.44		22.0	71.4	15.2	2.1
100	120	0.46	2.94		70.3	53.8	5.5	12.5
error	1	0.03	0.15	0.25	0.81	0.4	0.4	0.4

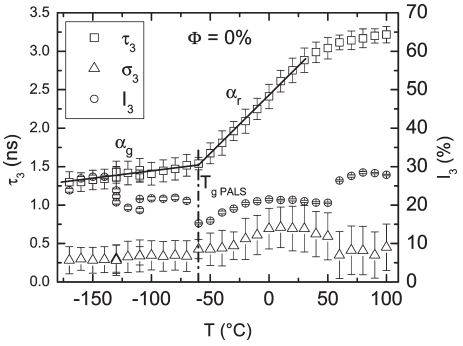

Figure 2. *o*-Ps lifetime τ_3 (squares), *o*-Ps dispersion σ_3 (triangles), and intensity I_3 (circles) as a function of temperature for the pure polymer temperature was kept constant at $T = -130$ °C for several measurements to check for a time dependence of the intensity (see text).

shell to thermal properties is rather small and beyond detection limit. On the other hand, Δc_p is reduced because of increased contribution of nanoparticles (mass of PEP polymer decreased) this is consistent with the straight line in Figure 1, which has no free parameter, as the fit starts with the heat capacity of the pure polymer (no filler) and has to end at $\Delta c_p = 0$ for the pure filler (100%) .

Positron Annihilation Lifetime Spectroscopy (PALS). In Table 3 a full set of data for all concentrations and for two temperatures is given for our evaluation method (τ_1 fixed to 125 ps, hence not listed and $I_1 = 100\%$; $I_2-I_3-I_4$, not listed)

In Figures 2 and 3 the *o*-Ps lifetime τ_3, the dispersion σ_3, and the intensity I_3 are shown as a function of temperature for two selected concentrations, i.e., 0 and 18 vol %, respectively. The data for the other concentrations look similar and are presented in the Supporting Information.

In the following paragraph, we will first discuss the data for these two typical sets of concentrations in detail, in particular with respect to effects already known from literature. Only then we will present all data in a summarized graph and discuss the dependence on filler concentration and the consequences thereof.

Error bars for the *o*-Ps lifetime and the *o*-Ps intensity are from statistics of the fit. We did some repeated measurements at 30 °C which showed the reproducibility of the experiments. The *o*-Ps lifetimes and the respective intensities at room temperature are within expected range for these polymers,[8,9] although a direct comparison with literature values is not possible, as to the present author's knowledge this particular

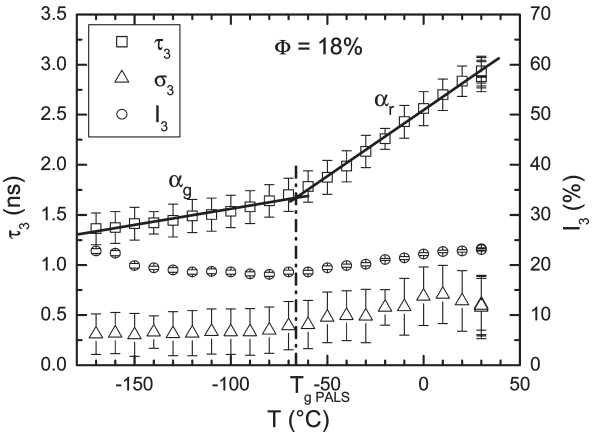

Figure 3. *o*-Ps lifetime τ_3 (squares), *o*-Ps dispersion σ_3 (triangles), and intensity I_3 (circles) as a function of temperature for a polymer–nanocomposite with 18% filler concentration.

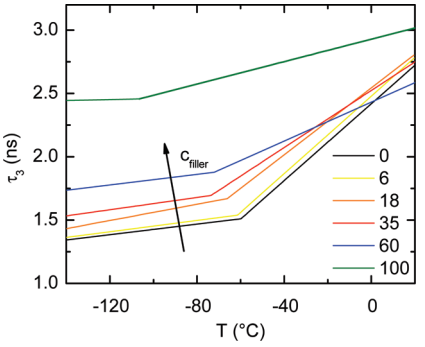

Figure 4. Overview of the temperature dependence of *o*-Ps lifetimes for all the measured concentrations. For the sake of clarity, only fitted straight lines through the data are shown.

polymer has not been investigated yet. As for the lower concentration of filler and temperatures below the respective glass transition temperature, the *o*-Ps intensity becomes time dependent, a phenomenon well-known and explained in literature.[8,9] We would like to remark that for the sake of clarity only the intensities at higher temperatures are compared, where these phenomena do not occur.

The temperature dependence of the *o*-Ps lifetime (squares) shows two changes in slope. One at higher temperature, frequently named knee temperature. This is well-known in the literature[9,20] and attributed to the fact that the time scale for the measurement (some ns) is on the same order of magnitude as the structural relaxation time of the polymer matrix; hence, the holes to be detected are not stable on the time scale of the measurement. We omitted this temperature range in the following presentation of the data for the sake of clarity. A second change in slope is located around the glass transition temperature, which is also reflected in the dispersion. This is also well-known[20,35] and reflects the change in microscopic thermal expansion at the caloric glass transition temperature. Qualitatively, the general behavior does not change with increasing filler concentration, as seen in Figure 3 for 18% of filler.

Figure 4 shows a comparison of the *o*-Ps lifetimes for all nanocomposites with different filler concentrations. One notes that at temperatures below the glass transition, the *o*-Ps lifetimes and hence the average hole sizes at fixed temperature increases with increasing concentrations. Also the glass transition shifts to lower temperatures. It is, in particular, striking that all the curves run parallel below T_g but have different

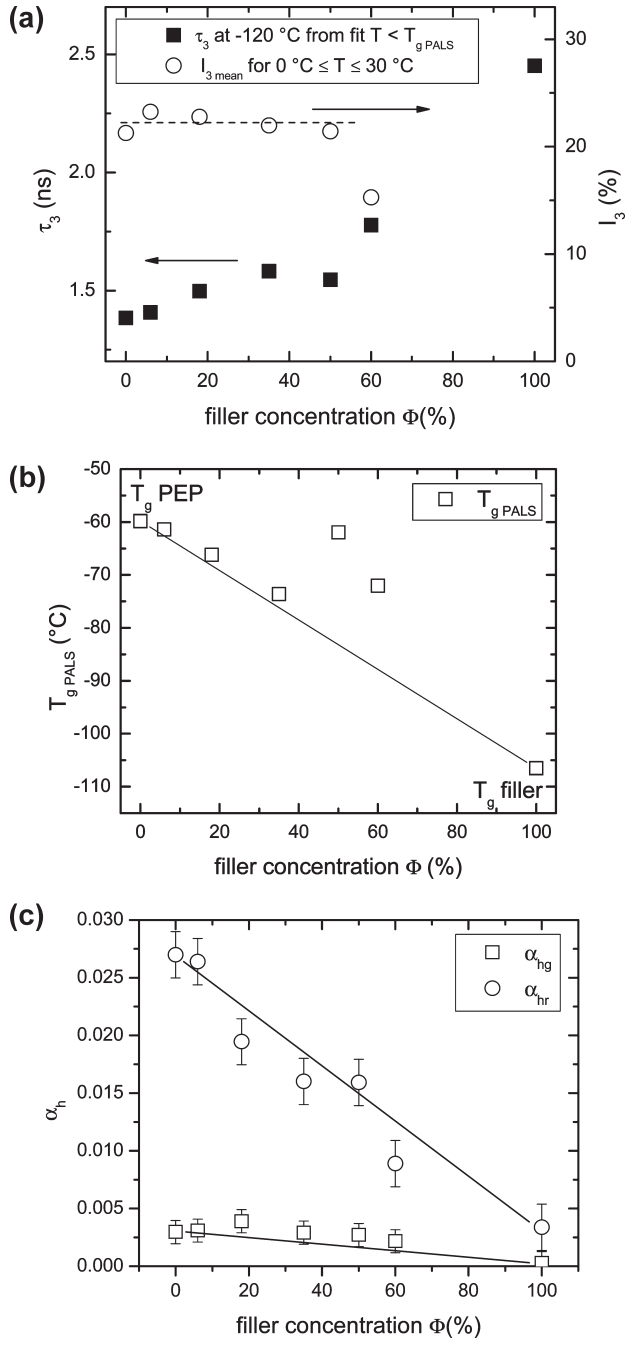

Figure 5. (a) τ_3 at −120 °C (squares, left-hand scale) and I_3 (circles, right-hand scale) as a function of filler concentration. (b) T_g from PALS as a function of filler concentration. The straight line represents a simple mixing rule connecting the T_g values measured in the pure polymer and in the pure filler, where it originates from the functionalized hydrophobic shell. (c) Thermal expansion coefficient of the hole free volume from PALS, i.e., α_{hg} (squares) and α_h (circles), below and above T_g respectively. Error bars are estimates from linear fits to *o*-Ps data vs temperature data. The straight lines are simple connections between first and last respective data point.

slope above T_g and even intersect within the experimental range. To make this quantitative, we extracted τ_3 at −120 °C, the slopes below and above the glass transition temperature and the glass transition temperature itself as a function of concentration and summarized these quantities in Figure 5a−c.

The following observation from Figure 5a can be made and is easy to explain. One notes that τ_3 at T = −120 °C increases with increasing filler concentration. One explanation is similar to the phenomenon frequently observed for filled membrane polymers,[19] where the polymer structure is disturbed locally near the particles.. Even without direct interaction, this can lead to an increased volume around particles, which might not be in equilibrium.[20,21] The resulting reduction in the overall packing density causes an increase in free volume and hence an increase in the *o*-Ps lifetime with increasing filler concentration.

However, neutron scattering experiments on exactly the same samples show no change of conformation with increasing filler concentrations.[31] Whether the same arguments as above hold for the present investigation or are due to a more general phenomenon, will be discussed in the following section.

The following three observations from Figure 5 are unexpected and not obvious to explain: Figure 5a shows a nearly constant intensity with increasing filler concentration. This is in contrast to observations in the literature[20,21] and also contradicts a simple mixing rule, where the intensity should decrease with increasing filler concentrations due to the higher amount of nonpositronium forming nanoparticles.

Figure 5b shows a decrease in the glass transition temperature T_g—determined from the change of *o*-Ps lifetime with temperature—with increase in filler concentration. This is in contrast to the DSC results and needs a detailed explanation.

Figure 5c shows the microscopic coefficient of thermal expansion. This was calculated from the slope of the *o*-Ps lifetime vs temperature curves from Figure 4, separately for temperatures below and above T_g. The *o*-Ps lifetime was converted via eq 1 to hole volume and the respective slopes were normalized to the value at T_g as usual in literature.[6,35,36] It has to be emphasized that this thermal expansion coefficient of the average free volume is only proportional to the macroscopic coefficient of thermal expansion.[6] The values we determined are in the expected range for polymers.[35,36,6] However, α_{hg} for $T < T_g$ is independent of concentration, whereas α_h above T_g decreases with increasing filler concentration. This appears to be in contradiction to similar experiments in literature.[27] In contrast to DSC, for the relevant properties obtained from PALS, a simple mixing rule does not hold for the polymer fractions..

The idea for an explanation of the puzzling facts is that PALS does "see" preferentially, i.e., with a weight above the volume fraction, the functionalized hydrophobic surface layer. The reason for this might be that positrons implanted into the SiO_2 nanoparticles diffuse out of these particles and preferentially annihilate in the functionalized surface layer (thickness aprox. 1.3 nm[32]), either as positrons or as positronium. This is possible due to the small averaged diameter of the nanoparticles (17 nm, ref 30) compared to the diffusion distance of Ps in matter (up to 100 nm in crystalline metals[37]) and has also been considered in other publications. In particular for nanosized Si-particles out-diffusion has already been discussed in the literature.[38] This approach can explain the above-mentioned puzzling facts.

The *o*-Ps intensity I_3 stays constant, as the nanoparticles themselves are not detected by the positrons and hence do not contribute to annihilation events. All positrons that are injected into the nanoparticles diffuse out and form positronium in the functionalized hydrophobic surface layer. Therefore, the increasing nanoparticle concentration does not reduce the *o*-Ps formation.

Concerning the thermal expansion, the first and maybe oversimplified assumption is a weighted average where the masses of the matrix and of the SiO_2 particles with their

hydrocarbon layers are used as weighting factors and the expansion of the SiO_2 particles is neglected:

$$\alpha(T) = m_{PEP}\alpha_{PEP}(T) + (m_{hydrocabons} + m_{SiO_2})\alpha_{hydrocabons}(T) \quad (2)$$

Here α are the respective coefficients of thermal expansion and m the respective masses. The course of the glass transition temperature T_g as a function of the filler concentrations in Figure 5b can be understood in terms of the very low glass transition temperature of the short chained functionalized surface layer, which is far below that of the polymer, and the idea that the positrons see this layer preferentially. The glass transition temperature T_g is then a mixture of the glass transition of the two intimately mixed constituents.

The reason why this has not been observed in the previous papers, e.g. in refs 20 and 21, might be that we choose a system that provides advantageous features (i) a low interaction between filler and polymer and (ii) short chains. In particular, two major advantages are related to the low molecular weight: (a) The polymer has a finite center of mass diffusion and is therefore able to fill at least partially the voids between the filler particles, even at higher concentrations. (b) The size of the polymer coils is significantly smaller than the particle diameter. In other words, the end-to-end distance of the polymer coils is much smaller than the topological confinement length which is related to the particles size, see, for example refs 31 and 32. Therefore, there is enough space between the particles to be pervaded by the polymer. (iii) An unperturbed conformation of the PEP3k chains was observed after the particle contribution was thoroughly subtracted.[30]

In contrast to other work, we are therefore able to unequivocally attribute this result to the molecules grafted to the silica surface. Because of the compatibility of these molecules, no interphase layer of the polymer is visible, that is frequently assumed, e.g., to explain the mechanical properties,[4] at least concerning the free volume and the other experiments on the same model nanocomposites within the limit of resolution of the present techniques.[30−32]

Conclusions

A well characterized weakly interacting system of a short-chain PEP matrix and hydrophobically functionalized silica nanoparticles with different nanoparticle concentrations was investigated by positron annihilation lifetime spectroscopy and DSC to separate the influence of the functionalized hydrophobic surface layer of the nanoparticles from interphase phenomena. The T_g and Δc_p from DSC experiments could be explained by a simple mixing rule. Positron annihilation lifetime spectroscopy was used to determine local free volume hole sizes, their temperature dependence, the glass transition temperature and the microscopic coefficient of thermal expansion. The results can be interpreted only under the assumption that the positrons preferentially probe the functionalized hydrophobic surface layer of the nanoparticles due to out diffusion of the positrons from the nanoparticles. No evidence is found for an interphase layer with properties different from the polymer matrix. The experiments show the high sensitivity of PALS to free volume in polymer−nanocomposites.

Acknowledgment. Financial support by German research society (SPP 1369 Interfaces and Interphases, Project Ra-796/5-1) is acknowledged. Scientific discussion and hints to literature by Prof. G. Dlubek (Halle) are deeply acknowledged. Help with DSC measurements and manuscript preparation by Isabel Jonas is gratefully appreciated. The authors thank Dr. M. Q. Shaikh for careful reading of the manuscript.

Supporting Information Available: Figures showing the complete set of PALS data for all concentrations. This material is available free of charge via the Internet at http://pubs.acs.org.

References and Notes

(1) *Polymer nanocomposites*; Mai, Y.-W., Yu, Z.-Z., Eds.; Woodhead Publishing Ltd.: Cambridge, U.K., 2006.
(2) *Metal-polymer nanocomposites*; Nicolais, L., Ed.; Wiley-Interscience: Hoboken, NJ, 2008.
(3) Luginsland, H. D. *A review on the chemistry and the reinforcment of silica-silane filler systems for rubber applications*; Shaker Verlag: Aachen, Germany, 2002.
(4) *Reinforcement of Polymer Nano-Composites, Theory, Experiments and Applications*, Vilgis, T. A.; Heinrich, G.; Klüppel, M., Cambridge University Press: New York, 2009.
(5) *Polymers: chemistry and physics of modern materials*,3rd ed.; McKenzie, J., Cowie, G., Eds.; CRC Press: Boca Raton, FL, 2008.
(6) Dlubek, G.; Pionteck, J.; Rätzke, K.; Kruse, J.; Faupel, F. *Macromolecules* **2008**, *41*, 6125–6133.
(7) . *Materials science of membranes for gas and vapor separation*; Yampolskii,, Y. P., Ed.; Reprinted with corr.; Wiley: Chichester, U.K., 2007.
(8) *Positron annihilation in chemistry*, Mogensen, O. E., Ed.; Springer series in chemical physics 58; Springer: Berlin, 1995.
(9) *Principles and applications of positron & positronium chemistry*; Jean, Y. C., Mallon, P. E., Schrader, D. M., Eds.; World Scientific: River Edge, NJ, 2003.
(10) Emmler, T.; Heinrich, K.; Fritsch, D.; Budd, P. M.; Chaukura, N.; Ehlers, D.; Rätzke, K.; Faupel, F. *Macromolecules* **2010**, *43*, 6075.
(11) Jansen, J. C.; Macchione, M.; Tocci, E.; De Lorenzo, L.; Yampolskii, Y. P.; Sanfirova, O.; Shantarovich, V. P.; Heuchel, M.; Hofmann, D.; Drioli, E. *Macromolecules* **2009**, *42*, 7589–7604.
(12) Rätzke, K.; Shaikh, M. Q.; Faupel, F.; Noeske, P.-L. M. *Int. J. Adhes. Adhes.* **2010**, *30*, 105–110.
(13) W. Yave, W.; Car, A.; Peinemann, K.-V.; Shaikh, M. Q.; Rätzke, K.; Faupel, F. *J. Membr. Sci.* **2009**, *339*, 177–183.
(14) Tao, S. J. *J. Chem. Phys.* **1972**, *56*, 5499.
(15) Jean, Y. C. *Microchem Acta* **1990**, *42*, 72.
(16) Nagel, C.; Schmidtke, E.; Günther-Schade, K.; Hofmann, D.; Fritsch, D.; Strunskus, T.; Faupel, F. *Macromolecules* **2000**, *33*, 2242.
(17) Kansy, J. *Nucl. Instrum. Meth. A.* **1996**, *374*, 235.
(18) Rudel, M.; Kruse, J.; Rätzke, K.; Faupel, F.; Yampolskii, Y. P.; Shantarovich, V. P.; Dlubek, G. *Macromolecules* **2008**, *41*, 788.
(19) Kruse, J.; Rätzke, K.; Faupel, F.; Sterescu, D. M.; Stamatialis, D. F.; Wessling, M. *J. Phys. Chem. B* **2007**, *111*, 13914–13918.
(20) Winberg, P.; Eldrup, M.; Frans, H.; Maurer, J. *Polymer* **2004**, *45*, 8253–8264.
(21) Winberg, P.; Eldrup, M.; Pedersen, N. P.; van Es, M. A.; Frans, H.; Maurer, J. *Polymer* **2005**, *46*, 8239–8249.
(22) Merkel, T. C.; He, Z.; Pinnau, I.; Freeman, B. D.; Meakin, P.; Hill, A. J. *Macromolecules* **2003**, *36*, 8406–8414.
(23) Reference deleted in proof.
(24) Chen, H. M.; Jean, Y. C.; Lee, L. J.; Yang, J.; Huang, J. *Phys. Status Solidi* **2009**, *11*, 2397–2400.
(25) Dlubek, G.; De, U.; Pionteck, J.; Arutyunov, N. Y.; Edelmann, M.; Krause-Rehberg, R. *Macromol. Chem. Phys.* **2005**, *206*, 827–840.
(26) Winberg, P.; DeSitter, K.; Dotremont, C.; Mullens, S.; Vankelecom, I. F. J.; Frans, H.; Maurer, J. *Macromolecules* **2005**, *38*, 3776–3782.
(27) Harton, S. E.; Kumar, S. K.; Yang, H.; Koga, T.; Hicks, K.; Lee, H.; Mijovic, J.; Liu, M.; Vallery, R. S.; Gidley, D. W. *Macromolecules* **2010**, *43*, 3415.
(28) Zhang, J.; Chen, H.; Li, Y.; Suzuki, R.; Ohdaira, T.; Jean, Y. C. *Radiat. Phys. Chem.* **2007**, *76*, 172.
(29) Chen, H. M.; Lee, L. J.; Yang, J.; Gu, X.; Jean, Y. C. *Mater. Sci. Forum* **2009**, *607*, 177.

(30) Nusser, K.; Neueder, S.; Schneider, G. J.; Meyer, M.; Pyckhout-Hintzen, W.; Willner, L.; Radulescu, A.; Richter, D. *Macromolecules* DOI 10.1021/ma101898c.
(31) Schneider, G. J.; Nusser, K.; Willner, L.; Falus, P.; Richter, D., submitted 2010.
(32) Nusser, K.; Schneider, G. J.; Neueder, S.; Willner, L.; Farago, B.; Holderer, O.; Richter, D., manuscript in preparation.
(33) Richter, D.; Monkenbusch, M.; Arbe, A.; Colmenero *J. Adv. Polym. Sci.* **2005**, *174*, 1.
(34) Kruse, J.; Kanzow, J.; Rätzke, K.; Faupel, F.; Heuchel, M.; Frahn, J.; Hofmann, D. *Macromolecules* **2005**, *38*, 9638.
(35) Dlubek, G.; Shaikh, M. Q.; Rätzke, K.; Faupel, F.; Pionteck, J.; Paluch, M. *Chem. Phys.* **2009**, *130*, 144906.
(36) Dlubek, G.; Shaikh, M. Q.; Rätzke, K.; Faupel, F.; Paluch, M. *Phys. Rev. E* **2008**, *78*, 051505.
(37) Hautojarvi, P. *Topics in current physics 12*; Springer-Verlag: New York, 1979.
(38) Brandt, W.; Paulin, R. *Phys. Rev. Lett.* **1968**, *21*, 193.